Hindawi
Advances in Materials Science and Engineering
Volume 2022, Article ID 7489680, 12 pages
https://doi.org/10.1155/2022/7489680

Research Article

Effect of Substrate Material on the Electromagnetic Properties of the Photolithography Printed Antenna

Thiyaneswaran Balashanmugam,[1] **Aruna Devi Baladhandapani**,[2] **Palanivel Rajan Selvakumaran**,[3] **Dhanagopal Ramachandran**,[4] **Suresh Kumar Muthuvel**,[5] **Priyadharshini Sivaraj**,[6] **and Samson Alemayehu Mamo**[7]

[1]*Department of ECE, Sona College of Technology, Salem, Tamilnadu, India*
[2]*Department of ECE, Dr. N.G.P Institute of Technology, Dr. N.G.P. Nagar, Coimbatore, Tamil Nadu, India*
[3]*Department of ECE, M.Kumarasamy College of Engineering, Karur, Tamilnadu, India*
[4]*Department of ECE, Chennai Institute of Technology, Chennai, Tamilnadu, India*
[5]*Institute of Electronics and Communication Engineering, Saveetha School of Engineering, Saveetha Institute of Medical and Technical Sciences, Saveetha University, Chennai, Tamilnadu, India*
[6]*Department of ECE, Tamilnadu Engineering College, Coimbatore, Tamilnadu, India*
[7]*Department of Electrical and Computer Engineering, Faculty of Electrical and Biomedical Engineering, Institute of Technology, Hawassa University, Awasa, Ethiopia*

Correspondence should be addressed to Samson Alemayehu Mamo; samson@hu.edu.et

Received 15 November 2021; Revised 26 April 2022; Accepted 29 April 2022; Published 1 June 2022

Academic Editor: V. Vijayan

In this study, a rectangular microstrip feed antenna on a fire-retarded substrate is presented. The antenna is designed using Computer Simulation Tool (CST) software. Different materials are used for the substrate, and the electromagnetic properties of the proposed structure are analyzed for each material. The EM property variation for each material is comparatively presented. The proposed antenna has CSRR (Complementary Split-Ring Resonator) which is engraved on the radiating element, and the shape of the CSRR is the hexagon. The proposed metamaterial-inspired antenna exhibits multiband operation at 2.1 GHz, 2.6 GHz, 4.6 GHz, 5.5 GHz, 6.1 GHz, and 7.1 GHz. With the help of material analysis, the fire-retarded substrate is chosen for the design, its excellent EM properties, and cheap cost. The photolithography-based printed antenna is validated with the help of S_{11}, VSWR, gain, directivity, surface current distribution, and radiation pattern. Simple, compact structure, good gain, stable radiation pattern, and excellent EM properties of the fire-retarded substrates make it suitable for the GHz application.

1. Introduction

The property of the materials used in the construction of any microwave device will directly affect the performance of the microwave device, the prerequisite for any microwave device design is the material selection knowledge. There are plenty of microwave materials available to manufacture microwaved devices, such as CNT, magnetic and ferrite materials, flexible materials, and metamaterials [1]. The selection of materials based on the range of operating frequency is another major requirement. There are a variety of microwave devices [2–4] such as antennas [5], filters, couplers, isolators, and mixers. Out of which, the antenna plays a vital role in all wireless applications. The antenna is a device made up of conductors that can convert the vibrating electrons into the EM signal during transmission and vice versa during the reception [6, 7]. Two decades before the antenna is of larger size; there are plenty of antennae-like dipoles, reflectors, slots, horns, etc. During the past two decades, there has been an enormous development in antenna design due to the development of wireless communication [8, 9]. The primary requirement of an antenna is compact size and multifunctionality. Both these essential requirements will depend on the antenna substrate. The amount of space

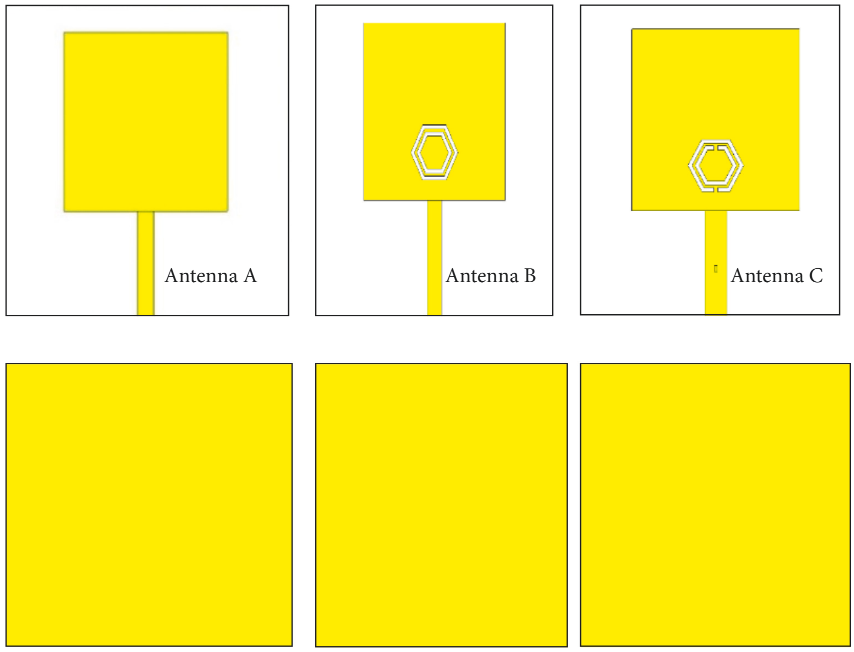

Figure 1: Evolution of HCSRR rectangular printed antenna.

Table 1: HCSRR rectangular printed antenna parameters in mm.

w	l	Wp	Lp	T	h
28	30	20	22	0.0035	1.6
a	b	s	wf	Lf	lg = *l*
8	5	0.5	2	10	36

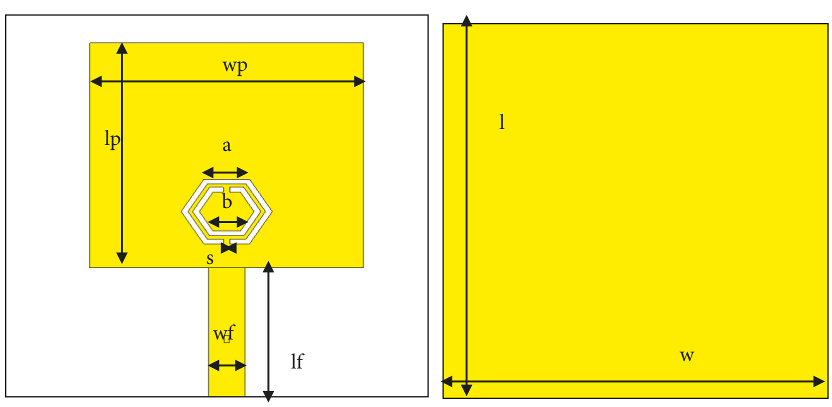

Figure 2: HCSRR rectangular printed antenna front and back view parameters.

available for the antenna in the present wireless devices is minimal, and they are utilized for multiple applications simultaneously. The size of the antenna will depend on the dielectric constant of the substrate material used.

Due to the compact size, ease of MIC (Microwave Integrated Circuits), integration, and efficiency at the GHz frequency of operation, the printed antenna [10–12] replaces the conventional antenna. The antenna has a conductive radiating element and ground. The substrate material is sandwiched between the radiating element and the ground. The radiating element, otherwise called the patch, is of any shape such as rectangular, square, circular, and triangular. The substrate materials that are widely used are Arlon, Roger, FR4, composite materials, magnetic materials, and other semiconductor materials [13, 14]. Another primary requirement for the antenna is the multiband functionality achieved with various techniques such as slotting, defected ground structures, integrating passive elements, and coupling patches. The major drawback of this type of technique is that it increases the design complexity [15] and affects the radiation pattern of the structures.

To overcome this drawback, researchers use metamaterials [16, 17] in the antenna structure. The materials with unnatural electromagnetic properties are considered

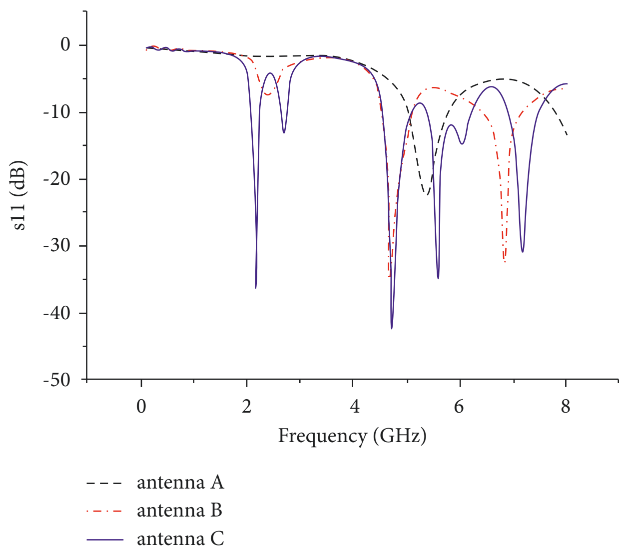

Figure 3: Comparison plot of antennas A, B, and C.

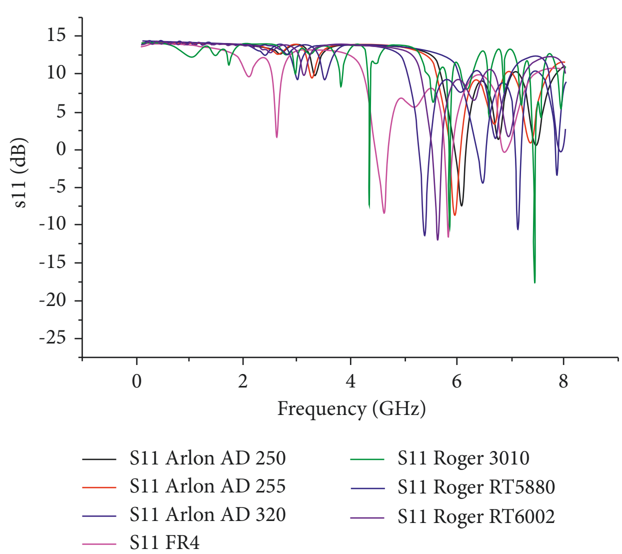

Figure 4: Return loss performance for various substrate materials.

Table 2: Various materials and their effects on electromagnetic properties.

Materials	No. of operating bands	Gain	Directivity
Arlon AD 250 C	1	2.6	5.2
Arlon AD 255 C	1	2.55	5.1
Arlon AD 320 A	1	2.8	5.6
Roger 3010	1	2.5	5
Roger RT5880	1	2.9	5.8
Roger RT6002	1	3.05	6.1
FR4	5	3.6	7.2

metamaterials. They have a negative refractive index, permittivity, and permeability. These properties are due to their periodic structure that satisfies the homogeneity property [18–23]. Various structures such as Split-Ring Resonator (SRR), Complementary SRR, Electric Inductive Capacitive (ELC), Complementary ELC, and many other structures

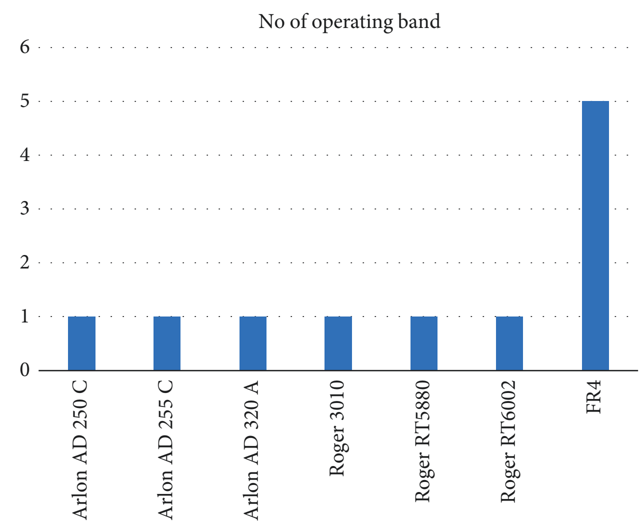

Figure 5: Number of operating bands for various materials.

exhibit the unnatural property [24, 25]. These materials are incorporated in the antenna to improve the antenna parameters [26–29] to achieve the wide bandwidth, improve impedance bandwidth, use as a superstrate to improve gain, and use the substrate to tune the radiation. However, the insufficient number of works available concerning the multiband operation uses the complementary split ring resonator.

In this study, a rectangular printed antenna inspired with hexagonal metamaterial is proposed for wireless application. The substrate for the design is FR4. The substrate is chosen based on the analysis of various substrates, and their results are presented. The critical parameters of the structure are finalized with the help of parametric analysis. In Section 2, the materials and methods used for the design are presented, followed by the result discussion in Section 3. In Section 4, the findings are concluded.

2. Materials and Methods

2.1. Design of the Multiband Metamaterial GHz Antenna. The proposed HCSRR rectangular printed antenna has a simple rectangular radiating structure. The entire structure is fed with a 50-ohm microstrip feed line. The proposed structure has three stages of evolution. The first stage is a simple microstrip patch antenna A; then, a two-ring hexagonal slot is introduced in the radiating element, which is termed antenna B, and finally, the slit in the hexagonal slot is introduced to design the HCSRR rectangular printed antenna. The proposed structure is fabricated on the FR4 substrate with a dielectric constant of 4.4. The substrate has the size of L x W x h mm^3. The radiating element and the feed line are printed on one side, and on the other side, the ground is printed. The feed, radiating element, and ground are made up of copper. In Figure 1, the evolution of the proposed metamaterial-inspired multiband antenna for GHz application [27, 28] is presented. The parameter values are presented in Table 1, and the final proposed structure along with its parameters is presented in Figure 2.

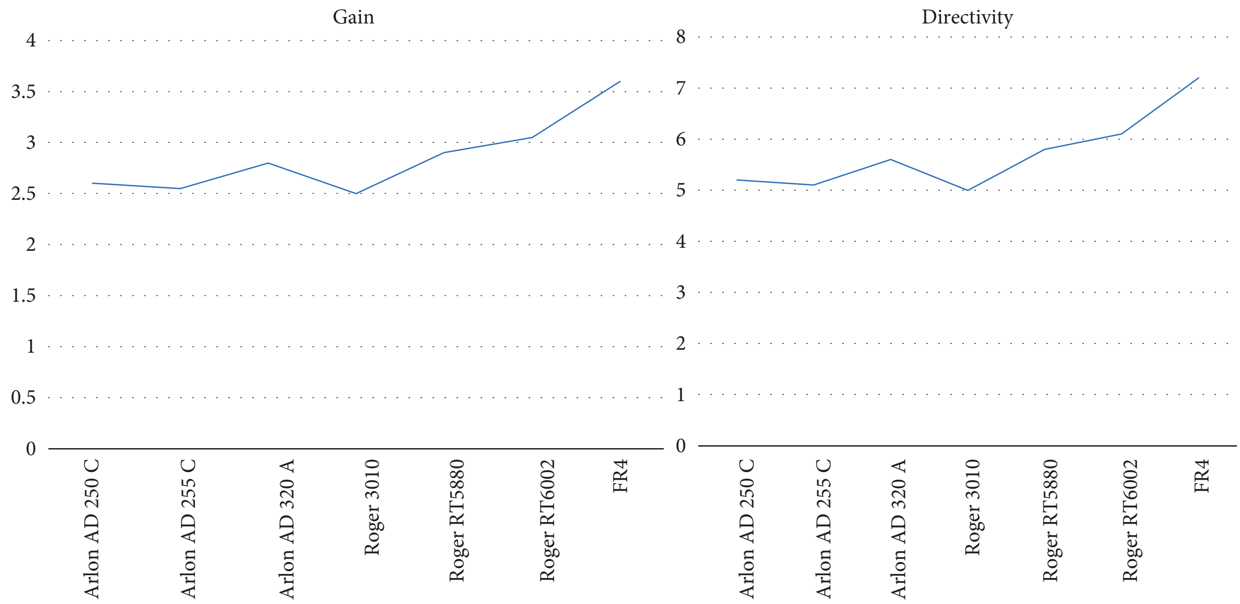

Figure 6: Gain and directivity for various materials.

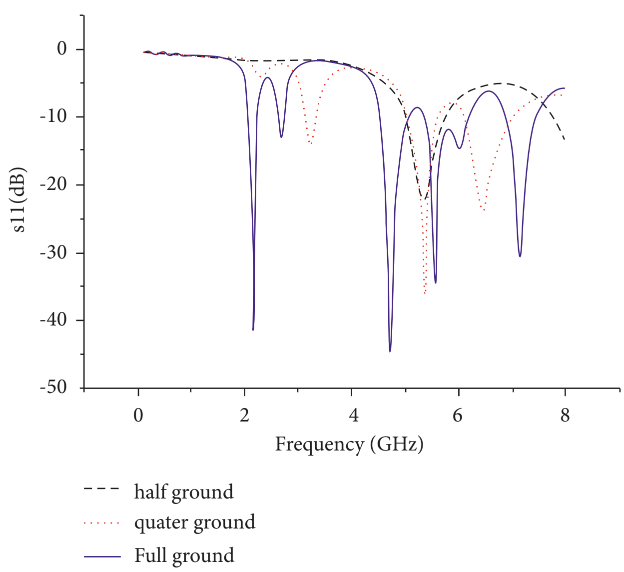

Figure 7: Return loss comparison concerning the various ground size.

The antenna A is a simple rectangular microstrip patch antenna designed to operate in a 5.2 GHz band. The designed structure operates in the frequency range of 5.00 GHz to 5.68 GHz resonating at 5.3 GHz. The return loss and the bandwidth are equal to 0.68 GHz and -24.18 dB. The antenna B is designed by introducing a dual-ring hexagonal slot in the radiating element precisely at the center concerning the substrate. With the introduction of the hexagonal slot, the current path direction is shifted, and as a result, with good impedance matching, the 5.3 GHz bands are shifted downward. The design antenna B is also a single band antenna that is operating at 4.6 GHz. The proposed structure's operating band is 4.52 GHz to 5.18 GHz with 0.66 GHz as bandwidth and -34.98 dB as return loss.

Then, the hexagonal complementary split-ring resonator is introduced in the radiating element, which enables the multiband characteristics of the proposed structure. The Antenna C resonates at 2.1 GHz, 2.6 GHz, 4.6 GHz, 5.5 GHz, 6.1 GHz, and 7.1 GHz. The proposed structure's operating band ranged from 2.08 GHz to 2.38 GHz, 2.58 GHz to 2.63 GHz, 4.52 GHz to 5.12 GHz, 5.32 GHz to 6.24 GHz, and 6.92 GHz to 7.46 GHz. In Figure 3, the comparison of various evolution antennas is presented. From this, we can observe that the metamaterial is the reason for multiband characteristics. The proposed structure operates five different resonating bands.

The antenna is designed using the following equation:

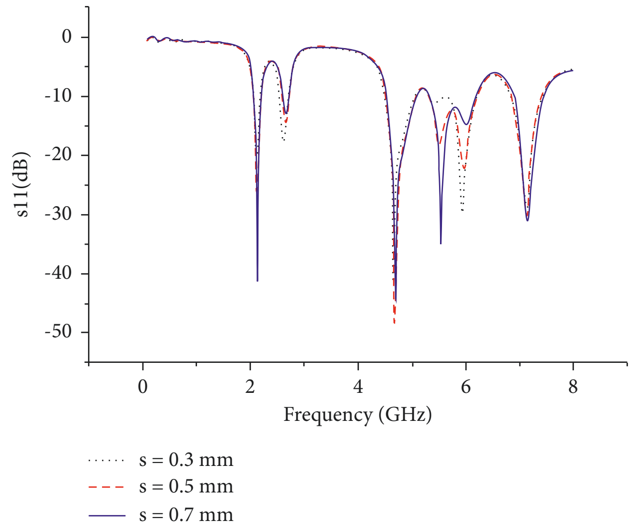

FIGURE 8: Return loss comparison for various split widths of HCSRR.

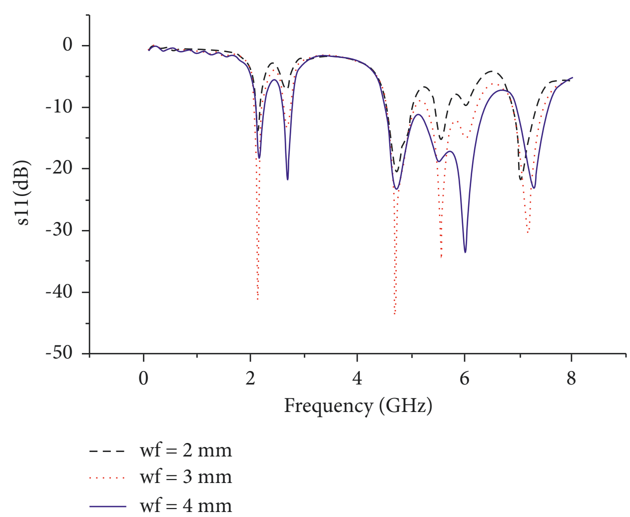

FIGURE 9: S_{11} for various feed width.

$$W = \frac{c}{2f_r}\sqrt{\frac{2}{\varepsilon_r + 1}},$$

$$L = \frac{c}{2f_r\sqrt{\varepsilon_{eff}}} - 2\Delta L,$$

$$\varepsilon_{eff} = \frac{\varepsilon_r + 1}{2} + \frac{\varepsilon_r - 1}{2}\left[1 + \frac{12h}{W}\right]^{-1/2}, \qquad (1)$$

$$\Delta L = 0.412h\,\frac{\left(\varepsilon_{eff} + 0.3\right)}{\left(\varepsilon_{eff} - 0.258\right)}\,\frac{(W/h + 0.264)}{(W/h + 0.8)},$$

where c is speed of light, f_r is resonant frequency, h is substrate height, and ε_{eff} is effective dielectric constant, respectively.

2.2. Substrate Material Analysis. The materials used as the substrate for the printed antenna design decide the proposed antenna's electromagnetic properties. Here, materials such as Arlon AD 250 C, Arlon AD 255C, Arlon AD 320 A, Roger 3010, Roger RT5880, Roger RT6002, and FR4 are analyzed as substrates. The simulated results are presented in Figure 4. From Table 2, we observe that the FR4 substrate can achieve a higher number of operating bands with decent gain and directivity. Therefore, the proposed antenna with FR4 material as the substrate can be used for wireless devices that can be utilized for multiple applications simultaneously.

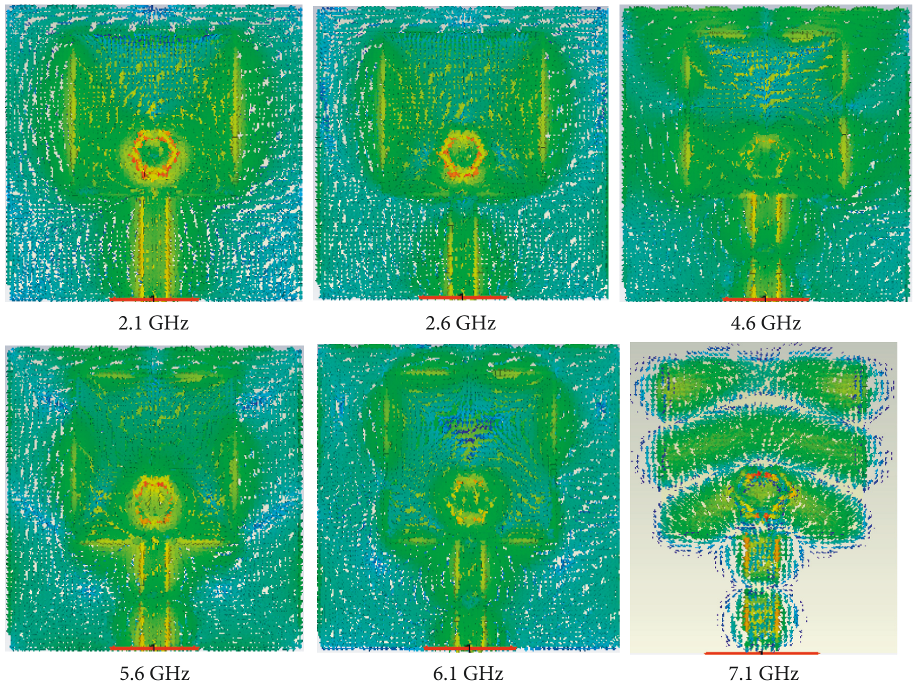

Figure 10: Surface current density plot at various resonating frequencies.

In Figure 5 (a), comparison of the number of operating bands is presented. In Figure 6, the gain and directivity of the proposed antenna structure when utilizing various types of substrate materials are presented. From Figure 6, we observe that the antenna has FR4 material as the substrate has good reasonable gain and directivity compared to the other materials used.

2.3. Parametric Study. The antenna's critical parameters are analyzed with the help of the parametric analysis of the CST software. The analysis helps identify the optimum dimension of the proposed structure; the critical parameters are the ground length L, feed width wf, and HCSRR split width s and are the critical parameters chosen. First, the ground length L is chosen; the ground length is varied in terms of full ground, half ground, and quarter ground. Out of the above combinations, the full ground can support the multiband characteristics in all operating frequencies with better matching of impedance. Therefore, for the final fabrication of the proposed structure, the complete ground is chosen. The response of s11 concerning various ground sizes is depicted in Figure 7. The split width of the hexagonal CSRR is increased from 0.3 mm to 0.7 mm in steps of 0.2 mm. The split width $s = 0.5$ mm has better matching, and it is the final value for the split width. The effect of the split width on the return loss is depicted in Figure 8, it is pragmatic that the higher resonant frequency is more affected, which evidences that the introduction of hexagonal CSRR is responsible for the higher-order resonant frequency. The feed width wf is augmented in stages of 1 mm from 2 to 4 mm. Feed width of 3 mm is capable of having excellent impedance around the operating bands as presented in Figure 9.

3. Results and Discussion

3.1. Effect of the Metamaterial Structure. HCSRR rectangular printed antenna's distributions of current at different operating frequencies are presented in Figure 10. It is observed from the figure that the current is evenly distributed over the entire radiating surface. At the frequency of 2.1 and 4.6 GHz, the current is concentrated on the hexagonal CSRR external ring. At 2.6 and 5.6 GHz, the current is concentrated more on the innermost ring. With the introduction of metamaterial structure, the current path is altered and enables the multiband characteristics of the proposed antenna.

3.2. Analysis of FR4 Substrate Printed Antenna. In Figure 11, the 3D radiation pattern, along with the E plane and H plane, is presented. At all frequencies except 6.1 GHz, the E plane radiation has a dipole radiation pattern. The proposed antenna H plane has an omni direction radiation pattern. At 6.1 GHz, the E plane has an end-fire pattern. It is observed from the three-dimensional radiation pattern that the exhaustive radiation is upright to the antenna.

In Figure 12, the HCSRR rectangular printed antenna's 11 characteristics are depicted, from which we can observe that the HCSRR rectangular printed antenna is operating at different bands. The VSWR of the proposed antenna at the operating frequency is less than 2.

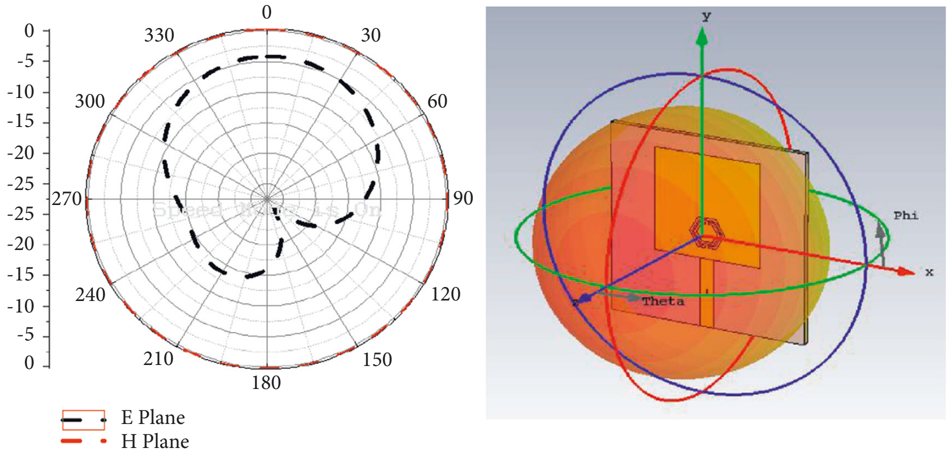

(a)

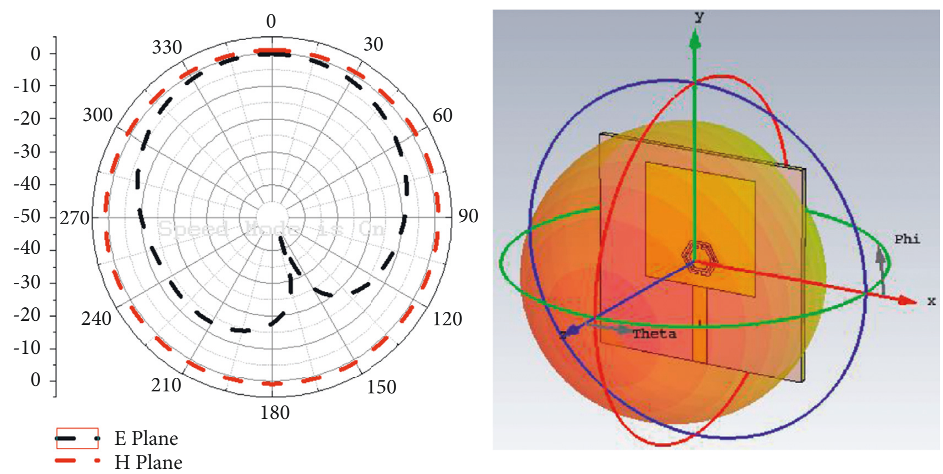

(b)

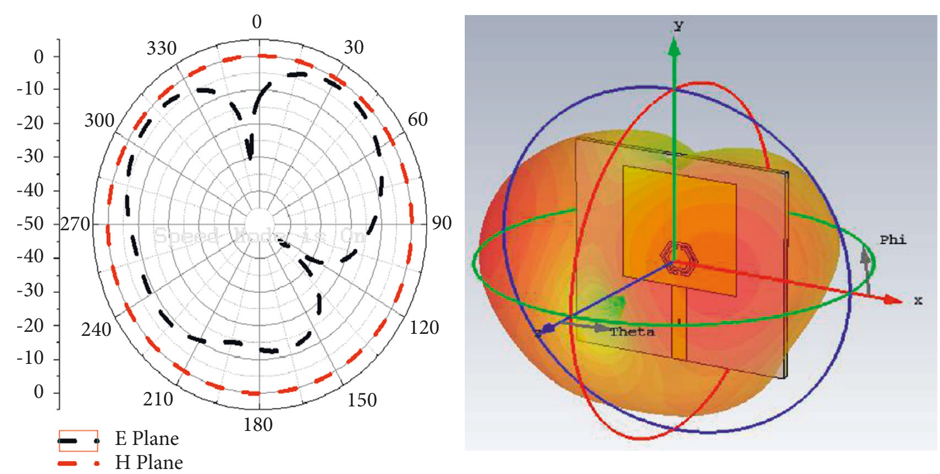

(c)

Figure 11: Continued.

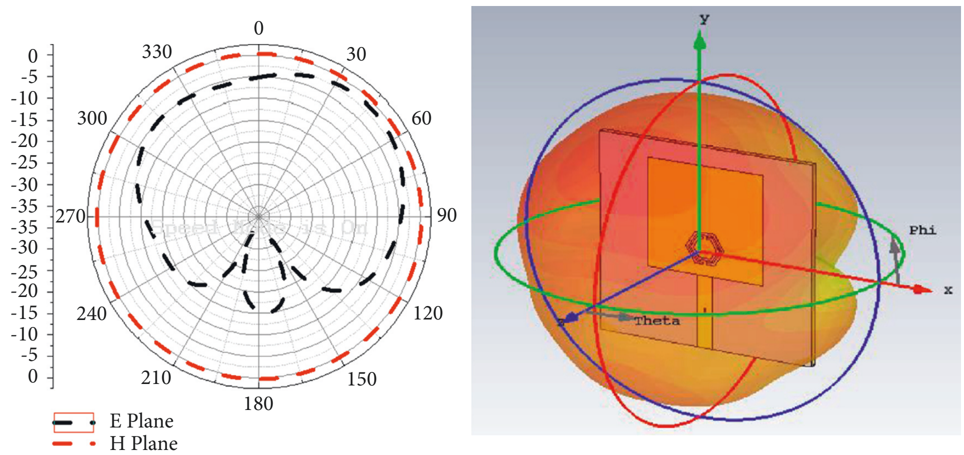

(d)

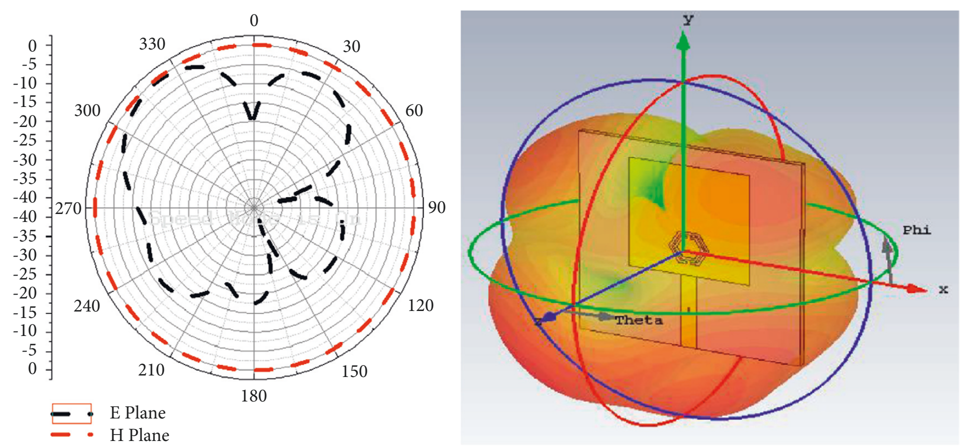

(e)

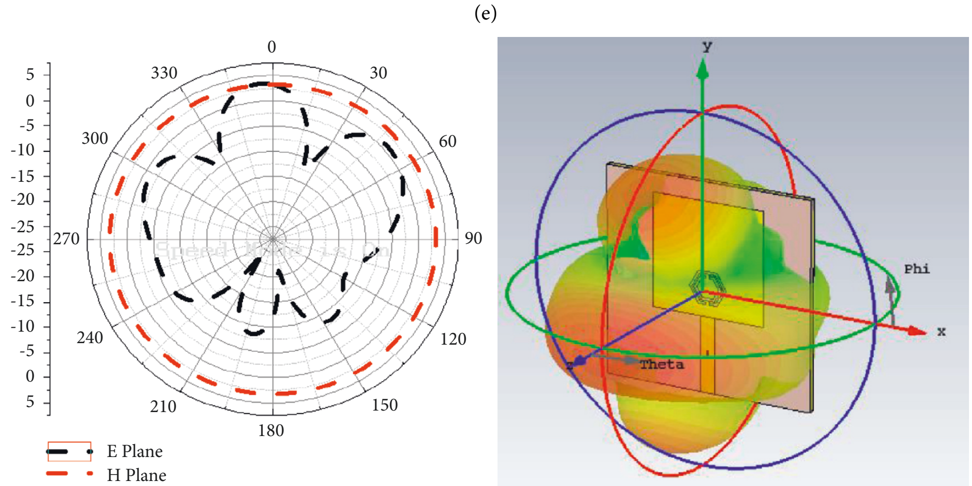

(f)

FIGURE 11: Radiation pattern at various resonating frequencies. (a) At 2.1 GHz, (b) at 2.6 GHz, (c) at 4.6 Hz, (d) at 5.5 GHz, (e) at 6.1 GHz, and (f) at 7.1 GHz.

In Figure 13, the directivity of the GHz antenna is presented. The maximum directivity is about 8 dB, and the directivity is above 5.4 dB in the entire operating region. In Table 3, the simulated result of the proposed metamaterial GHz antenna being tabulated.

3.3. Proof for Metamaterial Property. The designed CSRR is placed in a waveguide setup, as shown in Figure 14. An appropriate boundary condition is specified for the extraction of the transmission and reflection coefficient. Through the input port, the EM wave is used to excite the

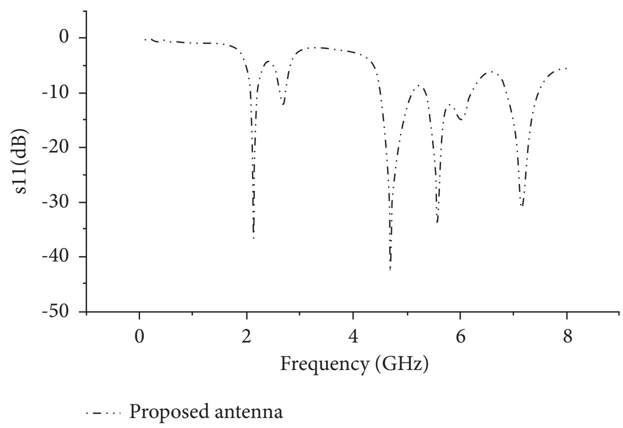

Figure 12: HCSRR rectangular printed antenna s11 characteristics.

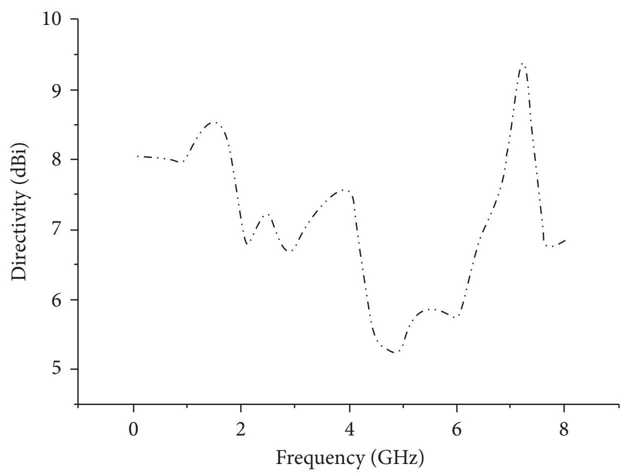

Figure 13: Directivity vs. frequency plot.

Table 3: Simulated result comparison.

Antenna	Operating band	Bandwidth (GHz)	Resonating frequency	Return loss	Gain (dB)	Directivity
A	5.00 GHz to 5.68 GHz	0.68	5.3 GHz	−24.18 dB	3.12	6.21 dB
B	4.52 GHz to 5.18 GHz	0.66	4.6 GHz	−34.98 dB	2.58	5.61 dB
C	2.08 GHz to 2.38 GHz	0.30	2.1 GHz	−41.28 dB	3.97	6.32 dB
	2.58 GHz to 2.63 GHz	0.05	2.6 GHz	−13.98 dB	2.89	6.89 dB
	4.52 GHz to 5.12 GHz	0.6	4.6 GHz	−44.28 dB	3.10	5.58 dB
	5.32 GHz to 6.24 GHz	0.92	5.5 GHz 6.1 GHz	−35.01 dB -15 .00 dB	1.86	6.00 dB 5.49 dB

CSRR, and at the output port, the *s* parameter coefficients are retrieved.

In Figure 15, the extracted S parameter is presented. From the figure, the reflection and transmission coefficient of the proposed antenna are presented. In Figure 16, the proposed antenna permittivity and permeability characteristics are presented. It is observed that the CSRR acts as an inductor; CSRR can have a permittivity value greater than 1 at the bands created by it. In Table 4, the proposed antenna is compared with the antennas in the literature.

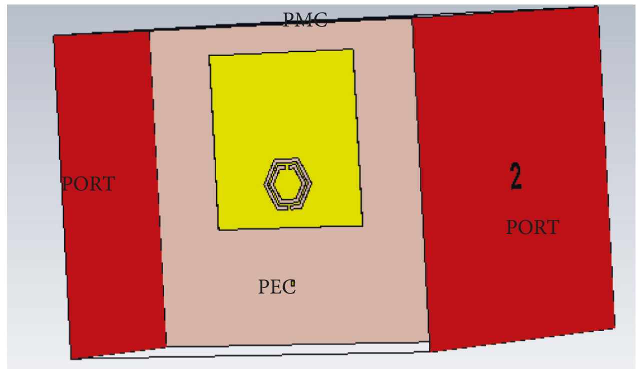

Figure 14: S parameter extraction setup.

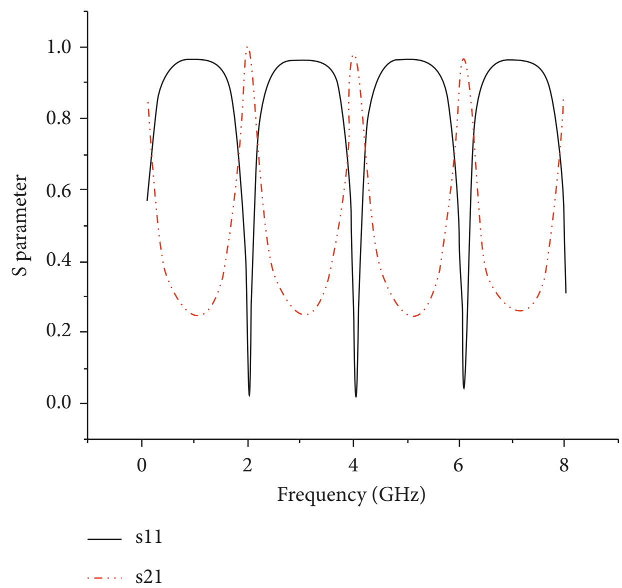

Figure 15: Extracted s11 and s21.

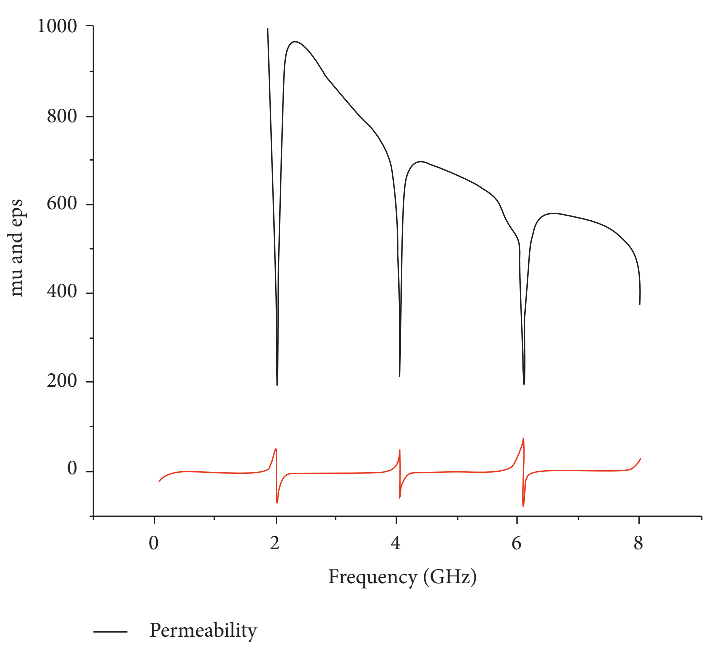

Figure 16: Permittivity and permeability characteristics.

Table 4: Proposed antenna vs. literature antenna.

Reference number	Technique used	Dimensions (mm)	No. of bands	Resonant frequency (GHz)	Equivalent circuit analysis	Metamaterial property verification
4	Slotted patch	25 × 25	2	2.41 to 6.10 and 9.40 to 13.81	Not presented	Not applicable
7	U-shaped patch with slot	30 × 30	2	3.31 to 3.60 and 5.10 to 6.00	Not presented	Not applicable
13	Slot	21 × 28	2	5.00 to 6.12 and 7.70 to 8.51	Not presented	Not applicable
21	Elliptical ring with split-triangular patch	30 × 33	2	2.52 to 2.62 and 3.31 to 3.64	Not presented	Not applicable
Proposed	CSRR	28 × 30	5	2.08 GHz to 2.38 GHz,2.58 GHz to 2.63 GHz,4.52 GHz to 5.12 GHz, 5.32 GHz to 6.24 GHz, and 6.92 GHz to 7.46 GHz	Presented	Presented

4. Conclusion

A rectangular hexagonal CSRR-inspired monopole antenna is presented. The antenna is designed on the substrate called FR4. The choice of the substrate is based on the material analysis and its effect on the electromagnetic properties. Here, materials such as Arlon AD 250 C, Arlon AD 255C, Arlon AD 320 A, Roger 3010, Roger RT5880, Roger RT6002, and FR4 are analyzed as substrates. Material analysis results are presented in Section 2, from which it is found that the proposed structure with FR4 as the substrate material is capable of achieving multiband functionality with reasonable gain and directivity. Metamaterial hexagonal complementary split-ring resonator is the reason for the multiband operation that can be validated with the help of the parametric analysis and surface current distribution. Five different operating frequencies, stable radiation patterns, and compactness make the proposed structure useful for the GHz application, such as material sensing, material characterizing, GHz, microwave, and communication applications.

Data Availability

The data used to support the findings of this study are included within the article. Further data or information can obtained from the corresponding author upon request.

Conflicts of Interest

The authors declare that there are no conflicts of interest regarding the publication of this paper.

Authors' Contributions

The authors confirm their contribution to the paper as follows: Dr. B. Thiyaneswaran, B. Aruna Devi, and Dhanagopal conceptualized and designed the study;S Palanivelrajan and Suresh Kumar Muthuvel collected data; S Priyadharshini, Samson Alemayehu Mamo, and B. Aruna Devi analyzed and interpreted the results; Dr. B. Thiyaneswaran, B. Aruna Devi, and S Palanivelrajan drafted and prepared the manuscript; Samson Alemayehu Mamo and B. Aruna Devi validated the study. All authors reviewed the results and approved the final version of the manuscript.

References

[1] Y. X. Liu, E. T. Kang, K. G. Neoh, J. F. Zhang, C. Q. Cui, and T. B. Thiam Beng Lim, "Surface graft copolymerization enhanced adhesion of an epoxy-based printed circuit board substrate (FR-4) to copper," *IEEE Transactions on Advanced Packaging*, vol. 22, no. 2, pp. 214–220, 1999.

[2] S. Fatima Farida, P. M. Hadalgi, P. V. Hunagund, and S. Rafath Ara, "Effect of substrate thickness and permittivity on the characteristics of rectangular microstrip antenna," in *Proceedings of the 1998 Conference on Precision Electromagnetic Measurements Digest (Cat. No.98CH36254)*, pp. 598-599, Washington, DC, USA, July 1998.

[3] A. Qureshi, M. U. Afzal, T. Tauqeer, and M. A. Tarar, "Performance analysis of FR-4 substrate for high frequency microstrip antennas," in *Proceedings of the 2011 China-Japan Joint Microwave Conference*, pp. 1–4, Hangzhou, China, April 2011.

[4] S. Baudha and V. D. Kumar, "Miniaturized dual broadband printed slot antenna with parasitic slot and patch," *Microwave and Optical Technology Letters*, vol. 56, no. 10, pp. 2260–2265, 2014.

[5] C. Caloz and T. Itoh, *Electromagnetic Metamaterials: Transmission Line Theory and Microwave Applications*, Wiley-IEEE Press, New York, 2005.

[6] D. H. Schaubert, D. M. Pozar, and A. Adrian, "Effect of microstrip antenna substrate thickness and permittivity: comparison of theories with experiment," *IEEE Transactions on Antennas and Propagation*, vol. 37, no. 6, pp. 677–682, 1989.

[7] K. Shan, C. L. Ruan, and L. Peng, "Design of a novel planar ultrawideband antenna with 3.5 and 5.5 GHz dual band-notched characteristics," *Microwave and Optical Technology Letters*, vol. 53, no. 2, pp. 370–375, 2011.

[8] K. Scheuer, J. Holmes, E. Galyaev, D. Blyth, and R. Alarcon, "Radiation effects on FR4 printed circuit boards," *IEEE Transactions on Nuclear Science*, vol. 67, no. 8, pp. 1846–1851, 2020.

[9] G. Geetharamani and T. Aathmanesan, "Design of metamaterial antenna for 2.4 GHz WiFi applications," *Wireless Personal Communications*, vol. 113, no. 4, pp. 2289–2300, 2020.

[10] K. Wei, J. Y. Li, L. Wang, R. Xu, and Z. J. Xing, "A new technique to design circularly polarized microstrip antenna by

fractal defected ground structure," *IEEE Transactions on Antennas and Propagation*, vol. 65, no. 7, pp. 3721–3725, 2017.

[11] P. Jones Christydass and N. Gunavathi, "Design of CSRR loaded multiband slotted rectangular patch antenna," in *Proceedings of the 2017 IEEE Applied Electromagnetics Conference (AEMC)*, Aurangabad, India, December 2017.

[12] K. Wei, B. Zhu, and M. Tao, "The circular polarization diversity antennas achieved by a fractal defected ground structure," *IEEE Access*, vol. 7, pp. 92030–92036, 2019.

[13] C.-y. Liu, T. Jiang, and Y.-s. Li, "A compact wide slot antenna with dual band-notch characteristic for ultra wideband applications," *Journal of Microwaves, Optoelectronics and Electromagnetic Applications*, vol. 10, no. 1, pp. 55–64, 2011.

[14] F. J. Herraiz-Martinez, G. Zamora, F. Paredes, F. Martin, and J. Bonache, "Multiband printed monopole antennas loaded with OCSRRs for PANs and WLANs," *IEEE Antennas and Wireless Propagation Letters*, vol. 10, pp. 1528–1531, 2011.

[15] P. Pingan Liu, Y. Yanlin Zou, B. Baorong Xie, X. Xianglong Liu, and B. Baohua Sun, "Compact CPW-fed tri-band printed antenna with meandering split-ring slot for WLAN/WiMAX applications," *IEEE Antennas and Wireless Propagation Letters*, vol. 11, pp. 1242–1244, 2012.

[16] A. T. Abed and A. M. Jawad, "Compact size MIMO amer fractal slot antenna for 3G, LTE (4G), WLAN, WiMAX, ISM and 5G communications," *IEEE Access*, vol. 7, pp. 125542–125551, 2019.

[17] S. S. Al-Bawri, S. Islam, H. Y. Wong, and M. F. Jamlos, "Bandwidth and gain enhancement of quad-band CPW-fed antenna for wireless applications," *Sensors*, vol. 20, no. 2, pp. 1–14, 2020.

[18] G. Dattatreya and K. K. Naik, "A low volume flexible CPW-fed elliptical-ring with split-triangular patch dual-band antenna," *International Journal of RF and Microwave Computer-Aided Engineering*, vol. 29, no. 8, 2019.

[19] A. Balanis, *Antenna Theory-Analysis and Design*, Wiley, Hoboken, NJ, USA, 3 edition, 2005.

[20] K. N. Paracha, S. K. A. Rahim, H. T. Chattha, S. S. Aljaafreh, S. u. Rehman, and Y. C. Lo, "Low-cost printed flexible antenna by using an office printer for conformal applications," *International Journal of Antennas and Propagation*, vol. 2018, pp. 1–7, 2018.

[21] A. Moradhesari, M. Naser-Moghadasi, and F. G. Gharakhili, "Design of compact CPW-fed monopole antenna for WLAN/WiMAX applications using a pair of F-shaped slits on the patch," *Microwave and Optical Technology Letters*, vol. 55, no. 10, pp. 2337–2340, 2013.

[22] Wa'il A. G. Al-Tumah and R. M. Shaaban, "Akeel Tahir, "Design, simulation and measurement of triple band annular ring microstrip antenna based on shape of crescent moon," *AEU - International Journal of Electronics and Communications*, vol. 117, 2020.

[23] C. Elavarasi and T. Shanmuganantham, "Multiband SRR loaded leaf-shaped Koch fractal with a modified CPW-fed antenna," *International Journal of Electronics Letters*, vol. 6, no. 2, pp. 137–145, 2017.

[24] A. Iqbal, A. Bouazizi, O. A. Saraereh, A. Basir, and R. K. Gangwar, "Design of multiple band, meandered strips connected patch antenna," *Progress In Electromagnetics Research Letters*, vol. 79, pp. 51–57, 2018.

[25] P. Ciais, R. Staraj, G. Kossiavas, and C. Luxey, "Compact internal multiband antenna for mobile phone and WLAN standards," *Electronics Letters*, vol. 40, no. 15, p. 920, Jul. 2004.

[26] S. Prasad Jones Christydass and N. Gunavathi, "Octa-band metamaterial inspired multiband monopole antenna for wireless application," *Progress In Electromagnetics Research C*, vol. 113, pp. 97–110, 2021.

[27] S. P. J. Christydass, J. Suganthi, S. Kavitha, and R. Yuvaraj, "Ring monopole antenna for Tera-Hertz application," *Materials Today Proceedings*, vol. 45, pp. 1827–1833, 2021.

[28] J.-L. Jaw and J.-K. Chen, "CPW-fed hook-shaped strip antenna for dual wideband operation," *Journal of Electromagnetic Waves and Applications*, vol. 22, no. 13, pp. 1809–1818, 2008.

[29] A. K. Gautam, L. Kumar, B. K. Kanaujia, and K. Rambabu, "Design of compact F-shaped slot triple-band antenna for WLAN/WiMAX applications," *IEEE Transactions on Antennas and Propagation*, vol. 64, no. 3, pp. 1101–1105, 2016.